Demonstration of Protection of a Superconducting Qubit from Energy Decay

Yen-Hsiang Lin, Long B. Nguyen, Nicholas Grabon, Jonathan San Miguel, Natalia Pankratova, and Vladimir E. Manucharyan

Phys. Rev. Lett. **120**, 150503 — Published 13 April 2018

DOI: 10.1103/PhysRevLett.120.150503

Demonstration of protection of a superconducting qubit from energy decay

Yen-Hsiang Lin, Long B. Nguyen, Nicholas Grabon, Jonathan San Miguel, Natalya Pankratova, and Vladimir E. Manucharyan[1]

[1]*Department of Physics, Joint Quantum Institute, and Center for Nanophysics and Advanced Materials, University of Maryland, College Park, MD 20742, USA.*

(Dated: March 19, 2018)

Long-lived transitions occur naturally in atomic systems due to the abundance of selection rules inhibiting spontaneous emission. By contrast, transitions of superconducting artificial atoms typically have large dipoles and hence their lifetimes are determined by the dissipative environment of a macroscopic electrical circuit. We designed a multi-level fluxonium artificial atom such that the qubit's transition dipole can be exponentially suppressed by flux tuning, while it continues to dispersively interact with a cavity mode by virtual transitions to the non-computational states. Remarkably, energy decay time T_1 grew by two orders of magnitude, proportionally to the inverse square of the transition dipole, and exceeded the benchmark value of $T_1 > 2$ ms (quality factor $Q_1 > 4 \times 10^7$) without showing signs of saturation. Dephasing time was limited by the first-order coupling to flux noise to about 4 μs. Our circuit validated the general principle of hardware-level protection against bit-flip errors and can be upgraded to the $0 - \pi$ circuit [P. Brooks, A. Kitaev, J. Preskill, Phys. Rev. A**87**, 052306 (2013)], adding protection against dephasing and certain gate errors.

Introduction. Circuit quantum electrodynamics (QED) is a leading platform for quantum information processing because of the naturally strong interaction between superconducting circuits and microwave photons [1, 2]. A drawback of strong interactions is energy decay. The coherence time of state-of-the-art transmons and their variants is currently limited by the surface loss to about 100 μs [3]. This in turn reduces gate fidelities and complicates the realization of quantum error correction (QEC) algorithms [4–7]. A tempting alternative to QEC is protection at the hardware level [8, 9]. Here the state of a qubit remains unchanged by the environment due to special symmetries and/or topologies of the underlying (typically many-body) host system Hamiltonian. This approach is particularly well suited for superconducting circuits because of the flexibility in constructing designer Hamiltonians out of inductors, capacitors, and Josephson junctions [10–13]. Topological quantum computing with quasiparticles of p-wave type superconductors is another example of this idea [14]. Irrespective of which approach appears more viable, the future quantum computer will likely combine error correction at both hardware and software levels [15].

Two types of errors need to be eliminated: bit flips (energy decay) and phase errors (dephasing). Simultaneous correction of both errors is hard because their operators do not commute. For this reason, early experiments on QEC focused on heavily simplified codes correcting bit-flips only [16, 17]. For hardware-level protection the challenge consists of building complex multi-junction circuits with conflicting constraints [18]. The few previous experiments obtained encouraging data results with Josephson "rhombi" circuits [19, 20], yet the demonstration of the superiority of a protected design over a conventional one, even with respect to a single error type, was still missing. A natural way forward is to simplify the circuit design and explore protection against bit-flips only, especially given that energy decay is the limiting factor for circuit QED. Here we accomplished this key step by harnessing the interplay between plasma oscillations and flux tunneling in a fluxonium circuit [21].

The principle behind protection of any quantum system against energy decay is as follows [8, 22]. The two qubit states must have weakly overlapping wavefunctions, such that the transition matrix element of any local operator is suppressed. In atomic physics, these are called transition dipoles. A protected superconducting qubit thus draws analogies to selection rule suppressed (or forbidden) transitions of natural atoms, which play crucial role, e.g., in atomic clocks [23]. However, it is not clear a priori if selection rules can help to extend lifetime of macroscopic superconducting systems. Circuit QED involving forbidden transitions has not been explored.

We designed circuit parameters to combine both "forbidden" transitions (small dipole associated with suppressed flux tunneling) and "allowed" transitions (large dipole associated with plasma oscillations) in a single artificial atom. Moreover, the transition dipoles can be flux-tuned without significantly modifying the frequency. We show that qubit transitions of a fluxonium can still dispersively interact with a cavity mode even if the transition dipole is zero. This purely longitudinal interaction occurs via the virtual excitation of the allowed transitions to higher circuit states. Using this novel effect, we measured the energy decay time T_1 of a qubit as a function of its transition dipole. A reduction of the dipole by a factor of 10 results in the enhancement of T_1 by a factor of 100, in full agreement with the textbook theory

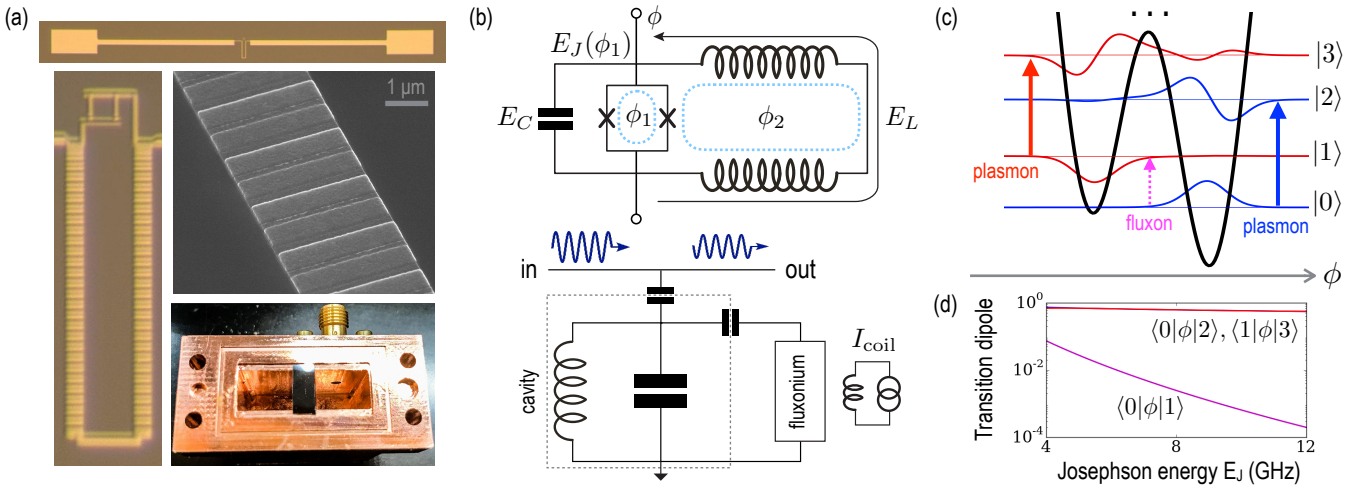

FIG. 1. (**a**) Images of a double loop fluxonium device in a 3D cavity. The antenna is directly connected to the split-junction. (**b**) Circuit models of a double-loop fluxonium atom (top) and its coupling to a 3D copper cavity (bottom). (**c**) Lowest 4 energy levels of the atom accurately positioned in the double-well potential profile, $U(\phi)$, along with their calculated wave-functions. (**d**) The inter-well *fluxon* transition $0-1$ (magenta arrow in (c)) has a vanishing transition dipole $\langle 0|\phi|1\rangle$ and hence is of the "forbidden" type. The intra-well *plasmon* transitions $0-2$ and $1-3$ (blue and red arrows in (c), respectively) by contrast have transition dipoles of order unity and are thus of the "allowed" type.

of spontaneous emission [24]. The energy decay quality factor Q_1 reached the value of $Q_1 > 4\times10^7$ ($T_1 > 2$ ms for a qubit at 3.3 GHz) without signs of saturation, surpassing the best environment-limited transmons by an order of magnitude.

Forbidden transition in a fluxonium. Compared to the original fluxonium, here we have replaced the single weak junction with a flux-tunable split-junction, which is required to separate frequency tuning from transition dipoles tuning. The circuit is now coupled capacitively to a 3D copper cavity using a mm-size antenna (Fig. 1a). The resulting modified fluxonium can also be viewed as a 3D transmon shunted by a large linear inductance of a Josephson array (Fig. 1b). The circuit Hamiltonian [25] is defined by the inductive energy of the Josephson chain E_L, the charging energy of the total capacitance E_C, and the variable Josephson energy of the split-junction $E_J(\phi_1)$, as well as by the two fluxes ϕ_1 and ϕ_2 piercing the split-junction and the main loops, respectively. The generalized flux ϕ in the inductance is a position-like quantum variable of the circuit (we take all fluxes in units of $\hbar/2e$). It moves in an effective potential given by $U(\phi) = E_L\phi^2/2 - E_J(\phi_1)\cos(\phi+\phi_J(\phi_1)-\phi_2)$, where $E_J(\phi_1)$ and $\phi_J(\phi_1)$ are given in Ref. [25]. Kinetic energy is given by the term $4E_Cn^2$, where $n=-i\partial_\phi$ is a momentum-like continuous variable conjugate to ϕ.

Two distinct transition types emerge in our circuit in the regime $E_L/E_J \ll 1$ and $E_J/E_C \gtrsim 10$. The former condition ensures that the potential $U(\phi)$ consists of multiple Josephson wells, whose depth and elevation are tuned by the external fluxes ϕ_1 and ϕ_2, respectively. The latter condition weakens quantum tunneling such that every low energy state of the circuit tends to localize inside a single well (Fig. 1c). The intra-well transitions are called *plasmons* by analogy with plasma oscillations in junctions. Similar transitions occur in a transmon [26], except that here a plasmon remains charge-insensitive even for a small value of E_J/E_C due to the inductive shunt [27]. The inter-well transitions are called *fluxons*. These are accompanied by a twist in the superconducting phase along the fluxonium main loop by 2π. A fluxon is analogous to the transition of a flux qubit [28], except that it is about 10^2-10^3 times less sensitive to flux noise due to the large number of junctions in the fluxonium loop [29]. As long as the two adjacent wells are offset against each other, the two states connected by a fluxon would have a vanishing overlap [30]. A fluxon is therefore a "forbidden" transition in the sense that any operator $O(\phi)$ would have an exponentially small matrix element for sufficiently large ratio E_J/E_C. By contrast, plasmons are "allowed" (Fig. 1d), because their transition dipoles, naturally defined as matrix elements of ϕ, are all near unity for a broad range of values of E_J/E_C [31].

Circuit QED with a forbidden transition. Because the transition dipole vanishes, the transverse interaction of a fluxon with a cavity mode at $E_J/E_C \gg 1$ is negligible. How could such a transition be explored within the framework of conventional circuit QED? We found that there is a purely dispersive longitudinal interaction between the two in the form of $H_{\rm int} = \chi\sigma_z a^\dagger a$, where a ($a^\dagger$) is the photon annihilation (creation) operator, and σ_z is the fluxonium Hamiltonian projected onto its two eigenstates connected by a fluxon [25]. The origin of a non-zero dispersive shift χ can be understood as follows.

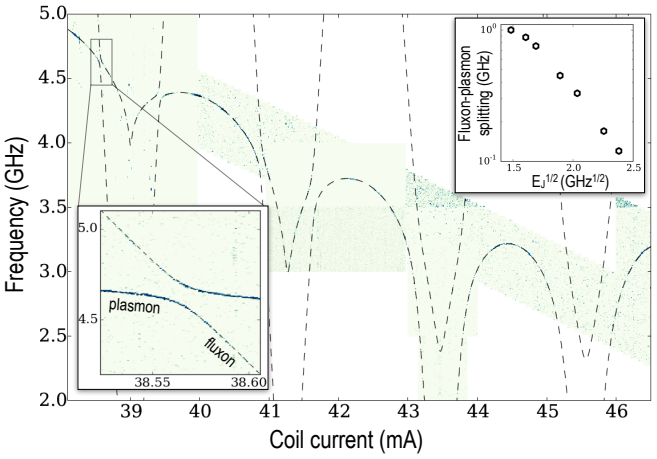

FIG. 2. Transmission near cavity resonance (scale not shown) as a function of the coil current and spectroscopy tone frequency. Cavity resonance is off the scale at about 10 GHz. Dashed lines represent a fit to the circuit model in Fig. 1b (see text). Left inset: a zoom-in on the smallest fluxon-plasmon splitting region. Right inset: measured values of the seven splittings visible in the plot vs. the extracted value of $E_J^{1/2}$ in frequency units.

In the state 0, which can be approximately viewed as the vibrational ground state of the lower well, fluxonium shifts the bare cavity resonance by an amount χ_0, due to virtual excitations of the lower well (blue) plasmon. The shift χ_0 grows as the plasmon frequency approaches the cavity resonance, and has a relatively large magnitude similar to that of a typical transmon qubit. Analogously, the state 1 shifts the cavity by an amount χ_1, due the higher well (red) plasmon. Since the lower and higher well plasmons have different frequencies, $\chi_0 \neq \chi_1$, giving rise to a non-zero dispersive shift $\chi = \chi_1 - \chi_0$. Quantitatively, the values of $\chi_{0(1)}$ are found by summing contributions from virtual excitations of every transition starting from the states 0(1), and in general there is no reason for the two to be equal [25, 32].

Model validation by spectroscopy. The spectrum of our artificial atom is revealed by a two-tone transmission spectroscopy signal measured as a function of the spectroscopy tone frequency and the current in the external coil that creates a global flux bias (Fig. 2). The readout tone was irradiated near the cavity's resonance at 10 GHz. Due to linearity of the coil, it is safe to assume that $\phi_{1,2} = \beta_{1,2} I_{\rm coil}$, where $I_{\rm coil}$ is the coil current and $\beta_{1,2}$ are flux couping constants. The two observed resonances vary with the coil current in a sophisticated quasi-periodic manner (Fig. 2). Nevertheless, the two fit remarkably well to the numerically-obtained lowest transitions of the circuit Hamiltonian involving only six adjustable parameters: $E_C, E_L, E_{J_1}, E_{J_2}, \beta_1, \beta_2$. Here $E_{J_{1,2}}$ are the Josephson energies of the two junctions in the SQUID. Transition dipoles can now be accurately calculated using the extracted model parameters [25].

Let us illustrate the essential spectral features of Fig. 2. The quasi-periodicity of the spectrum as a function of the coil current corresponds to changing the external flux in the main loop by a flux quantum, i.e. $\phi_2 \to \phi_2 + 2\pi$. The SQUID loop has a much smaller area and hence a much larger period. The point of inversion symmetry of the spectrum at $I_{\rm coil} \approx 45.5$ mA corresponds to biasing the SQUID loop with a half a flux quantum, i.e $\phi_1 = \pi$, and the Josephson energy $E_J(\phi_1 = \pi) = |E_{J_1} - E_{J_2}|$ reaches its minimum. The separation of the spectrum into fluxons and plasmons is particularly apparent in the region 38 mA $< I_{\rm coil} <$ 42 mA. The weakly flux-dependent transition with multiple sweet-spots (flat in external flux) is the lower-well plasmon. Due to the presence of the inductive shunt, plasmon's frequency is not a monotonic function of E_J, although it reduces with E_J on average. The transition that changes linearly with the coil current in a zigzag pattern is a fluxon. The avoided crossings correspond to a full hybridization of a fluxon with a plasmon (Fig. 2, left inset). The frequency splitting quantifies the strength of inter-well transitions, varying from 100 MHz at $I_{\rm coil} = 38.56$ mA, where a fluxon is well defined, to over 1 GHz near $\phi_1 = \pi$, where this notion becomes vague. The top inset of Fig. 2 illustrates that at sufficiently large values of E_J, the logarithm of the splitting scales as $E_J^{1/2}$, in agreement with the WKB description of tunneling.

Demonstration of protection. Controlled inhibition of energy decay in our circuit is most clearly demonstrated by measuring the lifetime of the lowest $0-1$ transition as we tune the coil current through the plasmon-fluxon anticrossing, shown in the lower inset of Fig. 2. Indeed, we observed a drastic enhancement of the T_1 time from $T_1 <$ 10 μs at the plasmon side to $T_1 > 1$ ms at the fluxon side (Fig. 3a). To interpret the data quantitatively, we turned to the model of dielectric loss, commonly encountered in transmon qubits [3]. This model echoes the observed enhancement of T_1 and requires the bounds on the effective loss tangent of the total capacitance shunting the split-junction to lie between $2 \times 10^{-5} < \tan\alpha < 2 \times 10^{-6}$. For the same range of coil currents, we plot the calculated dispersive shift χ, which remarkably does not drop significantly at the fluxon side of the anticrossing (Fig. 3b). The measured dispersive shift, extracted from the Rabi oscillations amplitude, agrees reasonably well with a theoretical expression [25], without adjustable parameters. In sharp contrast, the dispersive shift, calculated taking into account only the states 0 and 1, drops rapidly with the increase of T_1, emphasizing the importance of plasmons in creating the dispersive shift for fluxons.

Rabi oscillations along with π-pulse echo experiments demonstrate that a fluxon remains coherent even when its transition dipole suppressed to the extent that $T_1 >$ 1.5 ms (Fig. 3c). The coherence time T_2, given by the characteristic decay time of the echo signal, is given by $T_2 \approx 4$ μs, and is limited by the first-order flux noise

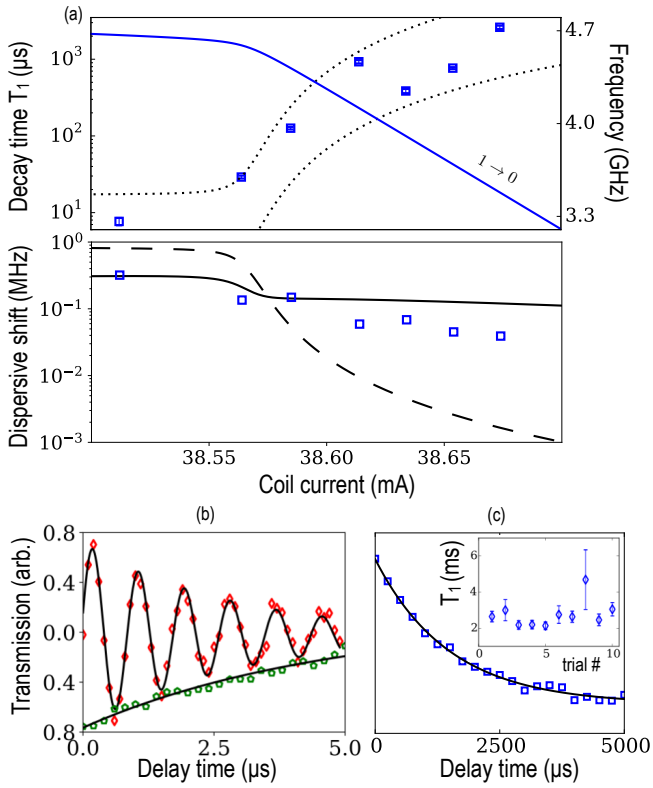

FIG. 3. (**a**) The measured lifetime T_1 of the $0-1$ transition (markers) and its frequency (solid line). Dotted lines are the dielectric loss prediction corresponding to the loss tangent values of 2×10^{-5} and 2×10^{-6}. Measured dispersive shift (blue markers) and calculated dispersive shifts, taking into account all transitions to higher levels (solid line) and only states 0 and 1 (dashed line). Note that χ decreases much slower than T_1 grows. (**b,c**) Example of time-domain data: Rabi oscillation trace (red), π-pulse echo trace (green), and energy relaxation trace (blue) all measured simultaneously with an interleaved pulse sequence. The inset shows repetitive measurements of T_1 during a period of about one hour.

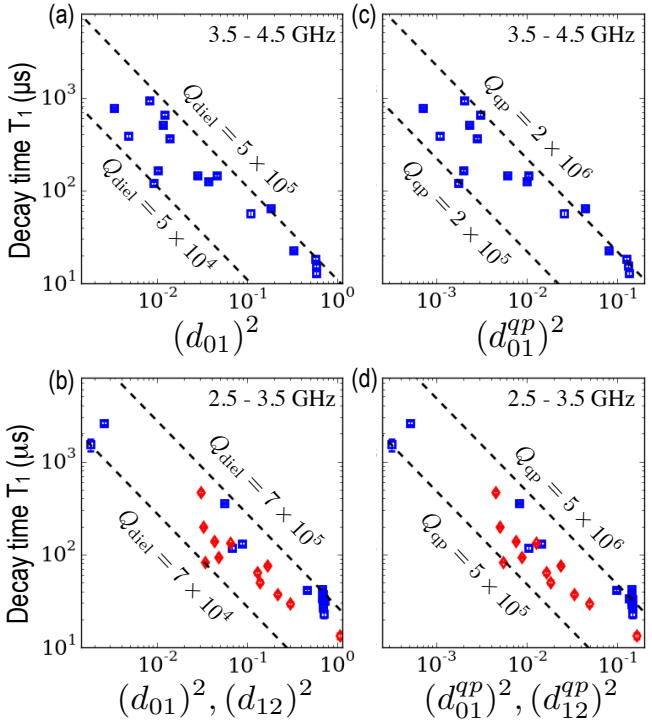

FIG. 4. Measured energy decay times for transitions $1-0$ (blue) and $2-1$ (red) taken from a narrow range of frequencies plotted against the calculated values of the corresponding transition dipole squared. Dashed lines illustrate Fermi's golden rule predictions for dielectric loss (**a,b**) and quasiparticle loss (**c,d**) using the expressions for their respective quality factors defined in [25]).

in the main loop, with a standard level of approximately $10^{-6}\ \Phi_0/\sqrt{\text{Hz}}$ at 1 Hz. The decay of the readout signal following a π pulse on a qubit fits the exponential function well and repeated experiments did not produce more than a factor of two variation of T_1 within about one hour (Fig. 3c - inset). This leads us to believe that the fluctuation of T_1 values in Fig. 3a occur on longer than a one hour time scale.

As a central point of our work, we have collected energy decay times for the qubit transition taken at a number of special values of I_{coil} such that the transition dipole d_{01}, given by $d_{01} = \langle 0|\phi|1\rangle$, vastly varies while the transition frequency is confined to a narrow interval $3.5-4.5$ GHz. All such transitions lose energy to essentially identical environments. Therefore, Fermi's golden rule predicts that at zero temperature $1/T_1^{1\to0} \propto (d_{01})^2$ for an arbitrary linearly-coupled environment. Our data obeys this simple scaling for the values of T_1 spanning a remarkable range of over two orders of magnitude (Fig. 4a). Despite some fluctuations, the data clearly shows that the dramatic enhancement of T_1 of a qubit occurs solely due to the reduction of its transition dipole. Because the suppression of d_{01} deep in the fluxon regime has no classical analog, the observed scaling evidences that the energy decay occurs by a spontaneous emission rather than by a thermal activation. Data for the neighboring $2.5-3.5$ GHz frequency range, including relaxation of the $2-1$ transition [25], confirms our conclusion (Fig. 4b).

The only known non-linear loss mechanism in which coupling to the bath cannot be described using the matrix elements of ϕ is quasiparticle tunneling across the small junctions [33, 34]. The effective transition dipole d_{ij}^{qp} responsible for the coupling to quasiparticles involves a more complex operator function of ϕ and depends on external flux [25]. However, replotting the energy decay times against this quantity (Fig. 4c,d) shows that coupling to quasiparticles is suppressed just as well as coupling to a linear bath. This is because a fluxon transition is forbidden from any local bath by the vanishing overlap of the qubit states wave functions (see Fig. 1c).

Conclusions. Suppression of transition dipoles necessarily decouples a qubit from both the external drive

and other circuits. The ultimate way around this is to perform gate operations in an unprotected regime and quickly return, e.g. by fast flux tuning, to the protected regime. An important component of the present work was our demonstration that dispersive coupling to a cavity mode can be arranged in the protected regime using transitions to higher states of the atom. As for the external driving, we used higher RF power to obtain sufficiently high Rabi frequency in the range $1-2$ MHz. We stress that this relatively slow Rabi frequency was due to an excessive (exponential in qubit-cavity detuning) filtering of the drive signal by a 3D microwave cavity, and can be improved in the future. For example, a recent work on a circuit similar to ours demonstrates the feasibility of a two-tone Raman driving of a forbidden transition [35].

Our experiment demonstrated for the first time that the energy decay time in a macroscopic artificial atom can be extended into the *ms* range by a controlled suppression of the overlap of the qubit state wavefunctions. Although the present scheme was not designed to protect against flux noise, we kept the condition $T_2 > 4\ \mu s$ at the most flux-sensitive spot thanks to the large inductance of fluxonium. Complete protection against flux noise can be tested by upgrading the present device to the Brooks-Kitaev-Preskill "$0-\pi$" qubit, which requires capacitive coupling of two fluxoniums with enhanced shunting inductors [13]. The current design can be utilized in experiments where moderate gate fidelity suffices but broad range tuning of transition frequencies and/or dipoles can be useful, for instance in quantum annealing or thermodynamics. During the review of this work an experiment on protected fluxoniums complimentary to ours [35] reported similar conclusions.

We thank Nathanaël Cottet for fruitful discussions and acknowledge funding from US National Science Foundation (DMR-1455261) and ARO-MURI "Exotic states of light in superconducting circuits".

[1] A. Wallraff, D. I. Schuster, A. Blais, L. Frunzio, R.-S. Huang, J. Majer, S. Kumar, S. M. Girvin, and R. J. Schoelkopf, Nature **431**, 162 (2004).
[2] R. J. Schoelkopf and S. M. Girvin, Nature **451**, 664 (2008).
[3] C. Wang, C. Axline, Y. Y. Gao, T. Brecht, Y. Chu, L. Frunzio, M. Devoret, and R. Schoelkopf, Appl. Phys. Lett. **107**, 162601 (2015).
[4] M. H. Devoret and R. Schoelkopf, Science **339**, 1169 (2013).
[5] J. Kelly, R. Barends, A. G. Fowler, A. Megrant, E. Jeffrey, T. C. White, D. Sank, J. Y. Mutus, B. Campbell, Y. Chen, *et al.*, Nature **519**, 66 (2015).
[6] A. D. Córcoles, E. Magesan, S. J. Srinivasan, A. W. Cross, M. Steffen, J. M. Gambetta, and J. M. Chow, Nature communications **6** (2015).
[7] N. Ofek, A. Petrenko, R. Heeres, P. Reinhold, Z. Leghtas, B. Vlastakis, Y. Liu, L. Frunzio, S. Girvin, L. Jiang, *et al.*, Nature **536**, 441 (2016).
[8] A. Y. Kitaev, Annals of Physics **303**, 2 (2003).
[9] C. Nayak, S. H. Simon, A. Stern, M. Freedman, and S. D. Sarma, Reviews of Modern Physics **80**, 1083 (2008).
[10] L. Ioffe and M. Feigelman, Phys. Rev. B **66**, 224503 (2002).
[11] B. Douçot, M. V. Feigel'man, L. B. Ioffe, and A. S. Ioselevich, Phys. Rev. B **71**, 024505 (2005).
[12] A. Kitaev, arXiv preprint cond-mat/0609441 (2006).
[13] P. Brooks, A. Kitaev, and J. Preskill, Phys. Rev. A **87**, 052306 (2013).
[14] J. Sau, Physics **10**, 68 (2017).
[15] J. Preskill, arXiv preprint arXiv:1203.5813 (2012).
[16] J. Chiaverini, D. Leibfried, T. Schaetz, M. D. Barrett, *et al.*, Nature **432**, 602 (2004).
[17] M. D. Reed, L. DiCarlo, S. E. Nigg, L. Sun, L. Frunzio, S. M. Girvin, and R. J. Schoelkopf, Nature **482**, 382 (2011).
[18] B. Douçot and L. B. Ioffe, Reports on Progress in Physics **75**, 072001 (2012).
[19] S. Gladchenko, D. Olaya, E. Dupont-Ferrier, B. Doucot, L. B. Ioffe, and M. E. Gershenson, Nature Physics **5**, 48 (2009).
[20] M. T. Bell, J. Paramanandam, L. B. Ioffe, and M. E. Gershenson, Phys. Rev. Lett. **112**, 167001 (2014).
[21] V. E. Manucharyan, J. Koch, L. I. Glazman, and M. H. Devoret, Science **326**, 113 (2009).
[22] L. B. Ioffe, M. V. Feigel'man, A. Ioselevich, D. Ivanov, M. Troyer, and G. Blatter, Nature **415**, 503 (2002).
[23] A. D. Ludlow, M. M. Boyd, J. Ye, E. Peik, and P. O. Schmidt, Rev. Mod. Phys. **87**, 637 (2015).
[24] S. Haroche and J.-M. Raimond, *Exploring the quantum: atoms, cavities, and photons* (Oxford university press, 2006).
[25] *See Supplementary Material*.
[26] J. Koch, T. M. Yu, J. Gambetta, A. A. Houck, D. I. Schuster, J. Majer, A. Blais, M. H. Devoret, S. M. Girvin, and R. J. Schoelkopf, Phys. Rev. A **76**, 042319 (2007).
[27] J. Koch, V. Manucharyan, M. Devoret, and L. Glazman, Phys. Rev. Lett. **103**, 217004 (2009).
[28] F. G. Paauw, A. Fedorov, C. J. P. M. Harmans, and J. E. Mooij, Phys. Rev. Lett. **102**, 090501 (2009).
[29] V. E. Manucharyan, N. A. Masluk, A. Kamal, J. Koch, L. I. Glazman, and M. H. Devoret, Phys. Rev. B **85**, 024521 (2012).
[30] A. J. Kerman, Phys. Rev. Lett. **104**, 027002 (2010).
[31] G. Zhu and J. Koch, Phys. Rev. B **87**, 144518 (2013).
[32] G. Zhu, D. G. Ferguson, V. E. Manucharyan, and J. Koch, Phys. Rev. B **87**, 024510 (2013).
[33] G. Catelani, J. Koch, L. Frunzio, R. J. Schoelkopf, M. H. Devoret, and L. I. Glazman, Phys. Rev. Lett. **106**, 077002 (2011).
[34] I. M. Pop, K. Geerlings, G. Catelani, R. J. Schoelkopf, L. I. Glazman, and M. H. Devoret, Nature **508**, 369 (2014).
[35] N. Earnest, S. Chakram, Y. Lu, N. Irons, R. K. Naik, N. Leung, J. Lawrence, J. Koch, and D. I. Schuster, arXiv preprint arXiv:1707.00656 (2017).